The photovoltaic effect in non-uniform quantum wires

1993 J. Phys.: Condens. Matter 5 6091

(http://iopscience.iop.org/0953-8984/5/33/018)

J. Phys.: Condens. Matter 5 (1993) 6091–6097. Printed in the UK

The photovoltaic effect in non-uniform quantum wires

L Fedichkin, V Ryzhii and V V'yurkov

Institute of Physics and Technology, Russian Academy of Sciences, Krasikov Street 25a, 117218 Moscow, Russia

Received 29 March 1993

Abstract. Photon-induced intersubband scattering in a quantum ballistic channel (QBC) is investigated. Our calculations show that light absorption in a QBC with a non-uniform narrowed end can lead to a photovoltaic effect. Using a mode-matching technique the photocurrent is obtained. The evaluated responsivity, detectivity and band width of the proposed photovoltaic detector are conducive to practical application.

1. Introduction

Current nanofabrication technology makes it possible to observe electron wave propagation such as electromagnetic waves in guided wave structures [1, 2]. The electrons in such systems are constricted in two dimensions so that both the constriction sizes are comparable with the Fermi wavelength of electrons. Usually the mean elastic free path of electron motion in the channel is sufficiently larger than the length of the channel itself [3].

In this paper we report our investigation of the possibility of conversion of the far-infrared (FIR) photosignal into an electric current using a quantum ballistic channel (QBC). Our study was encouraged by the fact that existing FIR detectors had some drawbacks. Single-quantum-well and many-quantum-well FIR photodetectors have attracted much attention recently. However, they have rather poor selectivity and are almost not tunable. A detector based upon the quantum Hall effect structure [4] which is tunable with the aid of a rather strong magnetic field is already known. A novel type of detector based on a QBC does not have the above mentioned disadvantages. Also its fabrication is attainable by modern technology [5, 6].

2. Detector description

The traditional split-gate structure [1, 2] with a constant or smoothly varying split width is not appropriate for FIR detector application because its photocurrent is very small. This is due to the conservation of the longitudinal momentum of an electron-absorbing photon in the channel. So the current through the ballistic channel under illumination is almost the same as in darkness.

We suggest a split-gate structure such as that in figure 1. The essential feature of the electrode shape is that it provides a long constant-width channel with a rather sharp asymmetric narrowing at its end so that the subband bottom versus longitudinal coordinate diagram is like that in figure 2. In other words the energy levels of the transverse motion quantization should vary appropriately along the channel. It should be noted that a QBC

0953-8984/93/336091+07$07.50

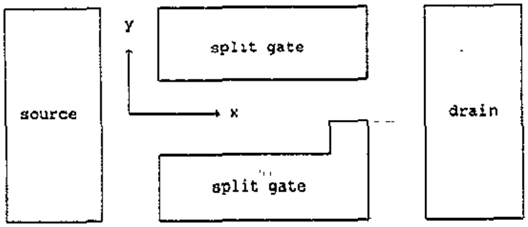

Figure 1. Configuration of contacts.

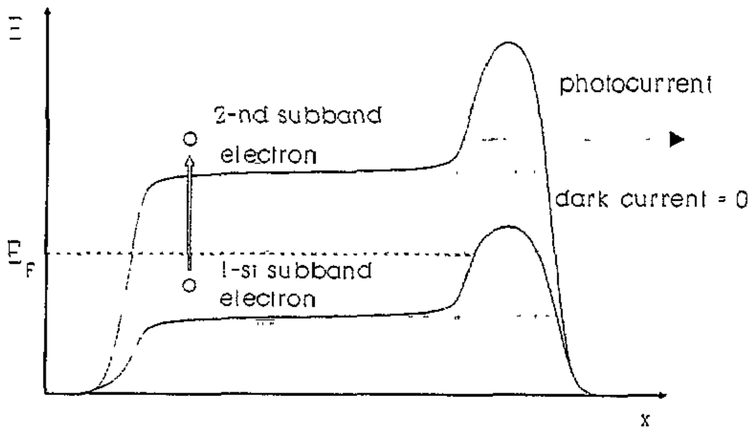

Figure 2. Subband diagram of the QBC versus the longitudinal coordinate x.

with such a form can be achieved by various technologies such as wet etching or ion-beam-induced damage isolation, and the split-gate technique enables us to tune the subband separation by applying a voltage to the split gate.

The main idea is as follows. Consider the case when only the lowest first subband in a wide channel is occupied by electrons, i.e. the first subband is under the Fermi level in a two-dimensional electron gas (2DEG) reservoir. There is a thick barrier for these electrons in a narrow channel; so the dark current is reduced to almost zero. The dark current caused by thermal activation or tunnelling is very small. When a photon has an energy $\hbar\omega$ close to the subband separation $\hbar\omega_0$ in the wide channel and is polarized perpendicular to the channel axis, an electron can absorb a photon and be excited to the second subband. There is a barrier for this electron in the narrow channel too. It cannot run through the barrier without leaving the second subband but, when the channel width variation in the intermediate region between two channels is rather sharp and asymmetric, a transition to the first subband is possible. In this way the electron can pass the narrow channel if its energy surmounts the first subband barrier height E_b. It occurs at least when E_b is higher than the Fermi energy E_F and lower than the subband separation $\hbar\omega_0$. In reality there is a simultaneous photon-assisted transition rather than two sequential processes of absorption and transition.

3. Calculation of structure characteristics

To evaluate the responsivity of the structure we have used a common perturbation theory for electron–photon interaction in a long-wave limit because we assumed the wavelength (about 50–250 μm) to be much greater than all the geometrical parameters of the structure. Even when the gate electrodes are opaque, the light can reach the channel because of diffraction. Gate electrodes are almost semitransparent for a wavelength of 50–250 μm. The perturbation term to the Schrödinger equation is

$$\hat{V}(\boldsymbol{r}, t) = -(\mathrm{i}e\hbar/mn_0)\exp(\mathrm{i}\omega t)\sqrt{2\pi N\hbar/\omega}\, \boldsymbol{e}_{\mathrm{p}} \cdot \nabla \tag{1}$$

where $\boldsymbol{e}_{\mathrm{p}}$ is the polarization direction ($|\boldsymbol{e}_{\mathrm{p}}| = 1$), N the number of photons in a unit volume, n_0 the refractive index of the semiconductor, m the electron effective mass and e the electron charge.

As usual the constrictive potential caused by the split gate is assumed to be parabolic [3, 7]:

$$U(x, y) = \tfrac{1}{2}m\Omega^2(x)[y_{\mathrm{c}}(x) - y]^2 \tag{2}$$

where the x axis is directed along the channel, the y axis lies in the plane of the structure too, the z axis is perpendicular to the heterojunction plane, and y_{c} is the channel centre coordinate. Following [8] we consider the two-dimensional Schrödinger equation

$$-(\hbar^2/2m)(\partial^2/\partial x^2 + \partial^2/\partial y^2)\psi + U\psi = E\psi \tag{3}$$

in the framework of the envelope function approximation [7]. In the wide part of the channel, $\Omega(x) = \omega_0 =$ constant, so the subband energy spectrum has an oscillatory equidistant form. The x dependences of Ω^2 and y_{c} in (2) describe a narrowing and bending, respectively, of the channel.

The probability $w_{nk,n'k'}$ of a transition from a state (n, k) with a subband number n and a wavenumber k in the x direction to a state (n', k') was calculated using the condition that the wavefunctions ψ_{nk} are normalized to unit linear density, that is

$$\int_{-\infty}^{+\infty} \mathrm{d}x \int_{-\infty}^{+\infty} \mathrm{d}y\, \psi^*_{nk}\psi_{n'k'} = \delta_{nn'}\delta(k - k') \tag{4}$$

where $\delta_{nn'}$ is the Kronecker symbol and $\delta(k - k')$ the Dirac delta function.

It differs from zero only for transitions to the adjacent subband with conservation of a wavenumber k and only for y polarization of incident light. It equals

$$w_{n+1,n} = (2nN/mn_0^2)\pi^2 e^2\delta(\omega - \omega_0). \tag{5}$$

Provided that there is an asymmetric narrowing in the channel an excited electron can transform into another subband electron. If its energy exceeds the barrier height in this subband, it can pass the channel and contribute to a photocurrent.

Our analysis of electron transmission through the bent area is based upon the mode-matching method, which has been developed for the mode transfer of electromagnetic waves in non-uniform waveguides with hard walls independently by Katzenelenbaum [9] and Schelkunoff [10]. This effect should be treated for clarity in the coordinates (p, q) connected with the channel geometry rather than in the rectangular coordinates (x, y). The

p axis lies in the centre of the channel and q is defined as a distance to the p axis. The bounding potential has the usual parabolic form

$$U(p,q) = \tfrac{1}{2}m\omega_0^2 q^2. \tag{6}$$

For smooth channel bending, i.e. for $k_F R \gg 1$ and $R\sqrt{m\omega_0/\hbar} \gg 1$, where $\hbar k$ is the longitudinal momentum and R is the radius of channel bending, the perturbation term to the two-dimensional Schrödinger equation can be written in the form

$$\hat{V}(p,q) = -(\hbar^2/2m)[1/R(p)](\partial/\partial q) \tag{7}$$

where $R(p)$ is the radius of channel bending.

We resolve the wavefunction $\psi(p,q)$ into a set of states with definite energy of transverse motion in the unperturbed Hamiltonian:

$$\psi(p,q) = \sum_{i=1}^{\infty} c_i(p) f_i(q) \tag{8}$$

where $f_n(q)$ (the normalized eigenfunction of the harmonic oscillator) obeys the equation

$$\partial^2 f_n/\partial q^2 = (2m/\hbar^2)[\tfrac{1}{2}m\omega_0^2 q^2 - \hbar\omega_0(n-\tfrac{1}{2})]f_n(q). \tag{9}$$

Substituting (8) into (3) and using (9) we obtain the infinite system of equations for transverse-mode coupling:

$$\partial^2 c_n/\partial p^2 + k_n^2 c_n = R^{-1}(p)\sqrt{m\omega_0/2\hbar}\sqrt{n}c_{n+1} - \sqrt{n-1}c_{n-1} \tag{10}$$

where $R^{-1}(p)$ is the channel curvature, k_n is defined as

$$k_n = \sqrt{(2m/\hbar^2)[E - \hbar\omega_0(n-\tfrac{1}{2})]} \tag{11}$$

and E is the electron energy.

It should be noted that only three amplitudes of adjacent modes are included in each equation (10). This effect arises from the properties of the parabolic bounding potential since in the generalized telegraphist equations [9, 10] dealing with hard-wall boundaries an infinite set of c_j occurs on the right-hand side of each equation corresponding to equation (10).

In the zero-order approximation there is no mode coupling, the excited electron is reflected from the barrier, and therefore we have for the wavefunction of the electron the following mode amplitudes:

$$c_{n\neq 2} = 0 \tag{12}$$

$$c_2 = \sqrt{2}\theta(-p)\sin(k_2 p). \tag{13}$$

Here $\theta(x)$ is the step function ($\theta(x) = 0$ when $x < 0$ and $\theta(x) = 1$ when $x > 0$) and the coordinate origin is placed at the barrier.

In the first-order approximation the amplitude of the transformation $2 \to 1$ can be calculated:

$$t_{21} = \frac{1}{2k_1}\sqrt{\frac{m\omega_0}{\hbar}}\int_{-\infty}^{0}\frac{\mathrm{d}p}{R(p)}\sin(k_2 p)\exp(\mathrm{i}k_1 p). \tag{14}$$

The effect of quantum reflection arises only in the next order of the above-mentioned parameter. It should be noted that the effect of mode coupling was applied previously to explain the experimental results in [5].

The transfer coefficient T_{21} due to mode matching is related to t_{21} by the formula

$$T_{21} = (k_1/k_2)|t_{21}|^2. \tag{15}$$

To evaluate this effect in split-gate structures we use the model form of channel bending:

$$R(p) = \begin{cases} R & \text{if } -\frac{1}{2}\pi R < p < 0 \\ 0 & \text{in other cases} \end{cases} \tag{16}$$

and evaluate R as half the gate splitting.

The dependence of T_{21} upon k_2 for this case is shown in figure 3.

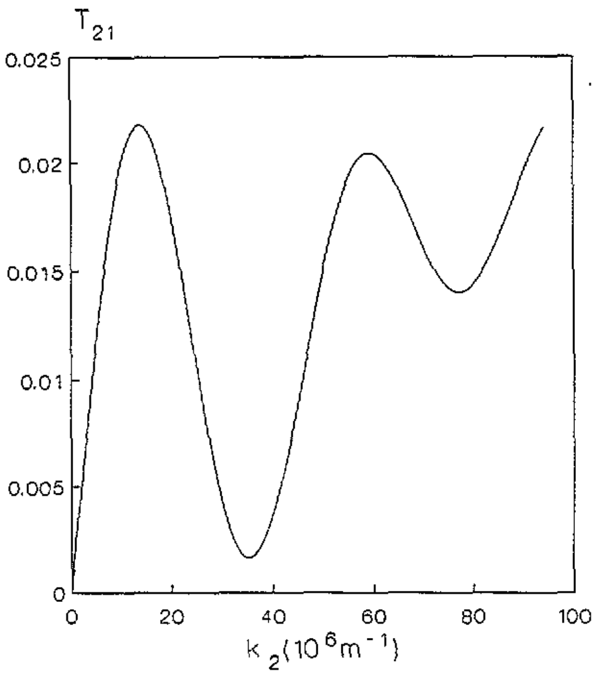

Figure 3. Transfer coefficient T_{21} versus the electron wavenumber k_2 ($\hbar\omega_0 = 5$ meV; $R = 50$ nm).

When the narrow split (figure 1) is less than about half of the wide split, the bending radius R is about half the average split width. The transformation efficiency according to (15) attains a value of about 0.014 for $h\omega_0 = 5$ meV and a split width of 0.1 μm. In fact for these conditions the transformation efficiency can be much greater (about unity as in [5]).

From (5) and (15) for the low-temperature limit, i.e. for $k_B T \ll E_F \simeq \hbar\omega_0$ (where k_B is the Boltzmann constant and T is the sample temperature) the ampere–watt responsivity R_λ was obtained:

$$R_\lambda = (4\pi L e^3/\hbar^2 S c\omega_0 n_0) v_F T_{av} \delta(\omega - \omega_0). \tag{17}$$

Here T_{av} is the averaged transfer coefficient given by the formula

$$T_{av} = \frac{1}{k_F}\int_0^{k_F} dk_2\, T_{21}(k_2). \tag{18}$$

L is the channel length, S is the structure area and v_F is the Fermi velocity.

For the usual split width of 0.3 μm the subband separation $\hbar\omega_0$ can be about 5 meV (the associated photon wavelength λ is about 250 μm). A split width of about 0.035 μm is already in reach [4]. The subband separation in this case approximately equals 15 meV ($\lambda \simeq 70$ μm). It should be emphasized that the subband separation can be fitted by the gate voltage.

For real channels the broadening $\Delta\omega$ should be taken into account. It is caused by various factors: scattering, rough gate electrode edges and finite channel length. So the δ-function in (5) should be replaced by the Lorentz function

$$f_L(\omega - \omega_0) = (1/\pi)\{\Delta\omega/[\Delta\omega^2 + (\omega - \omega_0)^2]\}. \tag{19}$$

A finite channel length L leads to a broadening $\Delta\omega/2\pi$ about a reciprocal transit time $\tau = L/v_F$. For ballistic channels, τ^{-1} should be greater than the scattering rate $\tau_{sc}^{-1} = v_F/l_s$ where l_s is the electron free path in the 2DEG. As for rough gate electrode edges they lead to much smoother channel width variations and therefore rather small broadening can be achieved. So the scattering sets the lower limit for $\Delta\omega$ when $L > l_S$. For a low temperature and a 2DEG density of 10^{11} cm^{-2}, $l_s = 10$ μm; so $\Delta\omega/2\pi$ is about 10^{10} Hz.

From (17) and (19) on the assumption that $\Delta\omega/2\pi = v_F/L$ a simple expression for the peak sensitivity of the detector was obtained:

$$R_\lambda = (2/\pi n_0)(e/\hbar\omega_0)(e^2/\hbar c)(L^2/S)T_{av}. \tag{20}$$

If we assume that $S = L^2$, $E_F = \hbar\omega_0 = 5$ meV and T_{av} is about unity, this expression gives R_λ equal to about 0.2 A W^{-1} which is close to that achieved previously [1,2]. However, the advantage of the proposed detector is convenient tuning by a gate voltage. The calculated dependence R_λ upon channel bending is shown in figure 4.

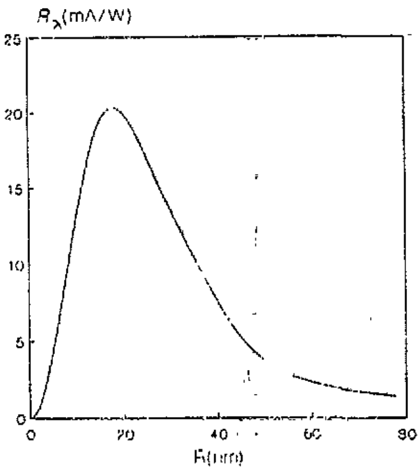

Figure 4. Responsivity of the structure versus the radius of channel bending ($\hbar\omega_0 = 5$ meV).

The response time is limited by the transit time τ.

We also estimate the detectivity determined by the thermal dark current since the tunnelling current may be suppressed by fabricating a thicker barrier. With the dark resistance σ^{-1} of the structure at zero bias being given by

$$\sigma^{-1} = (\pi\hbar/e^2)\exp[(E_b - E_F)/k_B T] \tag{21}$$

following [11] we obtain

$$\dot{D}_\lambda = (1/2e)R_\lambda\sqrt{S\pi\hbar/k_B T}\exp[(E_b - E_F)/2k_B T]. \tag{22}$$

For $\hbar\omega_0 = 5$ meV, $E_b - E_F = 5$ meV, $T = 4$ K, $S = 4 \times 10^{-12}$ m^2, and R_λ obtained from (20) at $R = 50$ nm the detectivity of the detector is 10^8 m s$^{1/2}$ W^{-1}.

4. Conclusion

Our calculations show that photon-induced electron scattering in non-uniform quantum wires can lead to an electric current at zero bias, i.e. to a photovoltaic effect. A highly selective tunable FIR detector based on a QBC with asymmetric narrowing was proposed. The sensitivity peak is at the photon energy equal to a subband separation which can be operated by a gate voltage. The detector is photovoltaic and rather fast. Another possible application of this effect is experimental study of the QBC itself.

References

[1] Wharam D A, Thornton T J, Newbury R, Pepper M, Ahmed H, Hasko D G, Peacock D C, Ritchie D A and Jones G A C 1988 *J. Phys. C: Solid State Phys.* **21** L209–13

[2] van Wees B J, van Houten H, Beenakker C W J, Williamson J G, Kouwenhoven L P, van der Marel D and Foxon C T 1988 *Phys. Rev. Lett.* **60** 848–51

[3] van Wees B J, Kouwenhoven L P, Willems E M M, Harmans C J P M, Mooij J E, van Houten H, Beenakker C W J, Williamson J G and Foxon C T 1991 *Phys. Rev.* B **43** 12431–53

[4] Dießel E, Müller G, Weiss D, von Klitzing K, Ploog K, Nickel H, Schlapp W and Lösch R 1991 *Appl. Phys. Lett.* **58** 2231–3

[5] Wu J C, Wybourne M N, Yindeepol W, Weisshaar A and Goodnick S M 1991 *Appl. Phys. Lett.* **59** 102–4

[6] Rooks M J, Eugster C C, del Alamo J A, Snider G L and Hu E L 1991 *J. Vac. Sci. Technol.* B **9** 2856–60

[7] Stern F, Laux S E and Frank D J 1988 *Surf. Sci.* **196** 101–6

[8] Nakazato K and Blaikie R J 1991 *J. Phys.: Condens. Matter* **3** 5729–40

[9] Katzenelenbaum B Z 1955 *Dokl. Akad. Nauk USSR* **12** 711–4

[10] Schelkunoff S A 1955 *Bell Syst. Tech. J.* **34** 995–1044

[11] Keyes R J (ed) 1980 *Optical and Infrared Detectors (Topics in Applied Physics 19)* (Berlin: Springer) pp 106–9